Heliyon 5 (2019) e01609

Contents lists available at ScienceDirect

Heliyon

journal homepage: www.heliyon.com

Heliyon

Synthesis and surface characterization of new triplex polymer of Ag(I) and mixture nucleosides: cytidine and 8-bromoguanosine

Lamia L.G. Al-mahamad *

Department of Chemistry, College of Science, Mustansiriyah University, Baghdad, Iraq

ARTICLE INFO

Keywords:
Inorganic chemistry
Materials chemistry
Analytical chemistry
Physical chemistry

ABSTRACT

In this work one-dimensional (1D) triplex polymer of silver (I): mixture nucleosides of cytidine and 8-bromoguanosine was synthesised. The polymer showed high stability due to the presence Ag(I) ions in the structure of the polymer in addition to the stability that produces from the effect of Hoogsteen hydrogen bonding in the triplex CGC. Atomic Force Microscopy (AFM) and transmission electron microscopy (TEM) were used to investigate the morphology of the polymer. The AFM images revealed formation of nanofibres extending many microns in length with height in the range of 2–3 nm. Statistical analyses carried out to analyse the AFM images to determine the height of the loops that formed in the polymer. The data displayed that the height value was in the range between 10 nm to 15 nm. The data of TEM images were consistent with the data of AFM images by displaying a very long fibre. Gwyddion software program was used to investigate surface parameters (roughness and waviness), diameter (size distribution), and probability density of the fibre. The data showed that the diameter of the fibre was ~0.4 nm.

1. Introduction

Based on the interactions of intermolecular hydrogen bonding, guanine and cytosine nucleobases can assemble to make long chains and forming networks, according to the known Watson-Crick pairing in both DNA and RNA [1]. Hydrogen bonding played an important role in the field of supramolecular chemistry [2] by forming different structures such as ribbons or fibres. Nucleobases and nucleosides are good examples of natural materials that depend on hydrogen bonding in their self-assembling. Another factor that helps forming larger structures in these compounds is the presence of multi binding sites in their structures [3] which increase the prone of these materials to self-assemble and produce structures of one dimension (1D), two dimensions (2D), and three dimensions (3D). Nucleobases and nucleosides showed attractive attention due to multifunctional properties of these structures such as conductivity [4], magnetism [5, 6], luminescence [7, 8], drug delivery, bioactivity, porosity [9], gas sensor, and nanotechnology [10]. Guanosine nucleoside has shown the ability to form G-quartet by self-assembling via hydrogen bonding [11]. Some of guanosine G-quartet were formed in the presence of metal ions such as K^+, Na^+, Ag^+, etc. [12], while others were formed in the absence of the effect of metal ions [13]. Triplex moiety is common in the reactions that involve guanosine and cytidine. Triplex structure consists of three triple structures where the third strand is binding to a duplex Waston-Crick purine strand, when the binding of the third strand occurs in an antiparallel way by reverse Hoogsteen hydrogen bonds; then the triplex is called purine motif (R), such as GGC, AAT, and TAT. In contrast, when the binding takes place in a parallel way via Hoogsteen hydrogen bonds, then this kind of triplex motif is called pyrimidine motif (Y), e.g., CGC, [14], Fig. 1 displays structures of R and Y. Both 8-bromo guanosine [15] and cytidine [16] showed the ability to form hydrogel with Ag(I) ions, while in triplex CGC no hydrogel was reported for these nucleosides with Ag(I) ion and this probably owing to the lack in the binding sites that occurs by forming triplex CGC with Ag(I) ion.

Studying surface roughness properties of the compounds, e.g., surface of semiconductor materials, is very important to know the changing that occurs on in the surface during the chemical reaction by forming or removing a layer from the surface. The atoms in the surface possess high chemical reactivity than that in the bulk as these atoms have the ability to alter their electronic structure by reaction with different kinds of chemical environments, these properties have found applications in different industrial technologies [17]. Semiconductor materials such as silicon and GaN characterise with high electron velocity and high electron mobility, and for this reason numerous researches have been

* Corresponding author.
E-mail address: Lamia.Almahamad@yahoo.com.

https://doi.org/10.1016/j.heliyon.2019.e01609
Received 3 December 2018; Received in revised form 4 March 2019; Accepted 26 April 2019

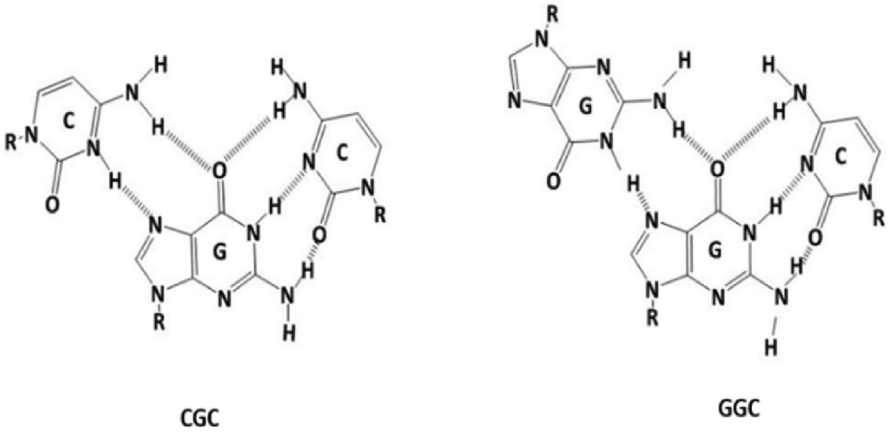

Fig. 1. Triplexes structures of parallel motif CGC (Y pyrimidine motif) and antiparallel motif GCG (R purine motif) bases.

reported to study the surface of these compounds which used in different applications such as electronics, optoelectronics, and sensors [18, 19, 20, 21]. In addition, in micro fluid devices, studying how the micro/nano scale influences in surface roughness is very important to develop devices with small-scale [22]. Here, one dimensional (1D) polymer of Ag(I) with a mixture of nucleosides: cytidine and 8-brpmoguanosine was prepared. The morphology of the polymer was characterised by using AFM and TEM techniques. The surface texture of the polymer was analysed with Gwyddion software program to indicate the statistical parameters of the surface roughness and to find the probability density, in addition to the diameter of the fibres. Preparing nanomaterial compounds with a large scale to use in nanotechnology applications still represents a hard task due to the difficulty controlling the synthesis process and the self-assembling of these compounds, as these compounds can change with the surrounding environment especially their chemical and stability properties rather than bulk materials [17]. Surface chemistry has the potential approach to solve this problem by understanding the relationship between physical-chemical properties of materials and their surface topography based on AFM characterizations, statistical analysis, and surface roughness analysis to provide better insight on the useful applications of these materials.

2. Materials and methods

2.1. Chemicals and materials

All chemicals were purchased from Sigma Aldrich and were used as received without further purification. ^{1}H and ^{13}C NMR spectra were performed on a Bruker Advance 300 spectrometer at 300 MHz, with DMSO-d_6.

2.2. Preparation silicon chips for AFM

P-silicon (100) wafers were used to achieve AFM measurements by cutting the wafers into 1 cm^2 and cleaning with 1:4 H_2O_2:H_2SO_4 (piranha solution) for 1 h, followed by washing the chips with deionised water and drying with nitrogen gas.

2.3. Atomic Force Microscopy (AFM) measurements

Sample for AFM measurements was prepared by drop-casting 2 μL of the sample onto 1 cm^2 clean silicon chip, then the sample was dried by air prior to scan with NanoScope Analysis 1.5 software (Bruker).

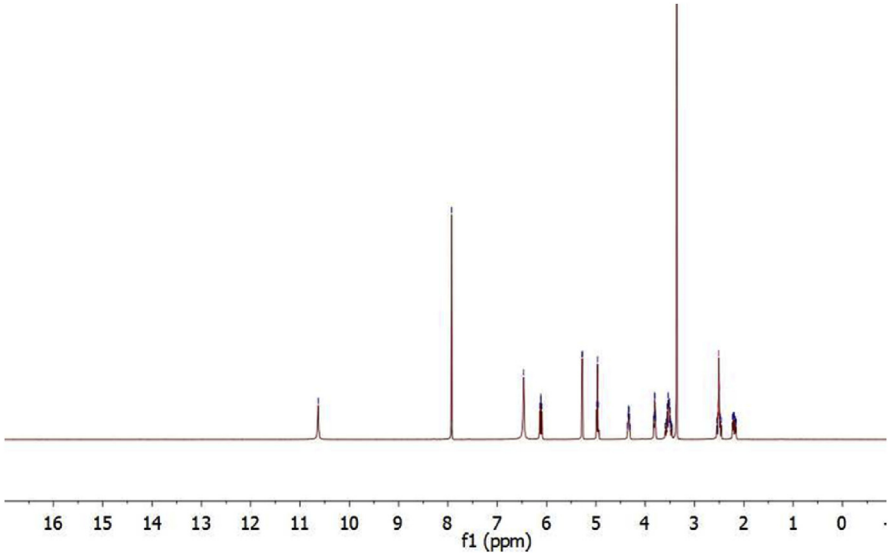

Fig. 2. ^{1}H NMR of guanosine in DMSO.

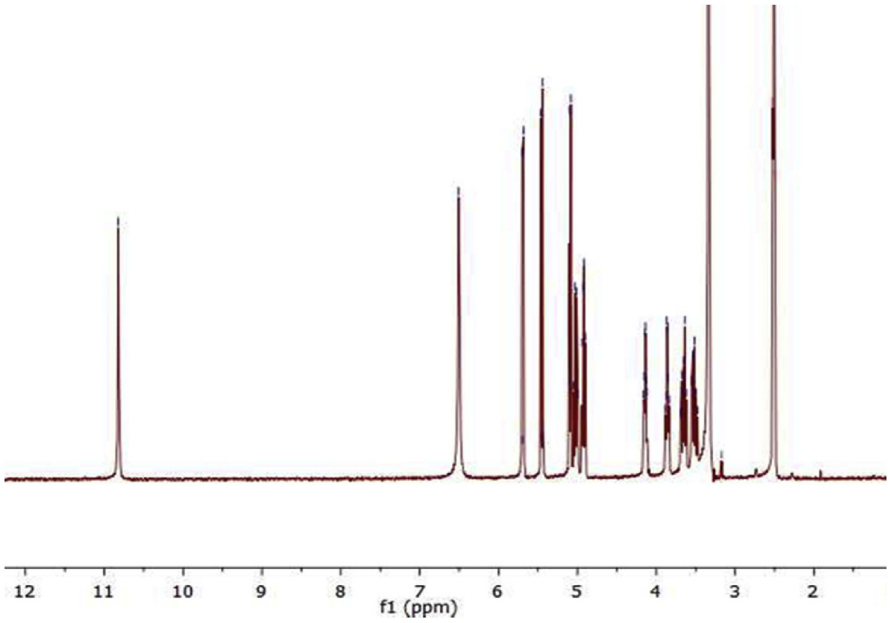

Fig. 3. ^{1}H NMR of 8-bromoguanosine in DMSO.

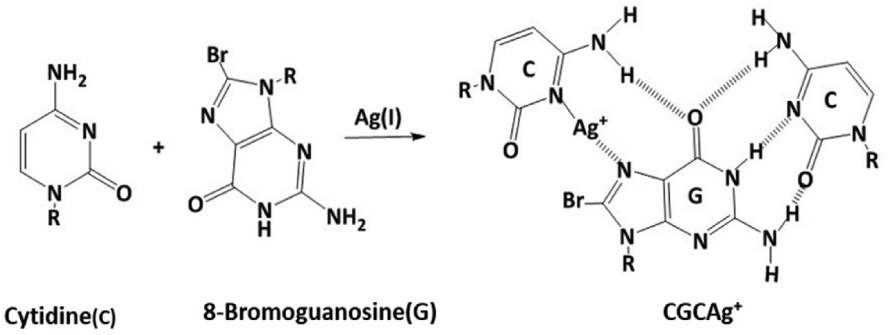

Fig. 4. Reaction scheme of cytidine (C) and 8-bromoguanosine (G) in the presence of Ag(I) ions for forming one dimensional polymer of triplex $CGCAg^{+}$.

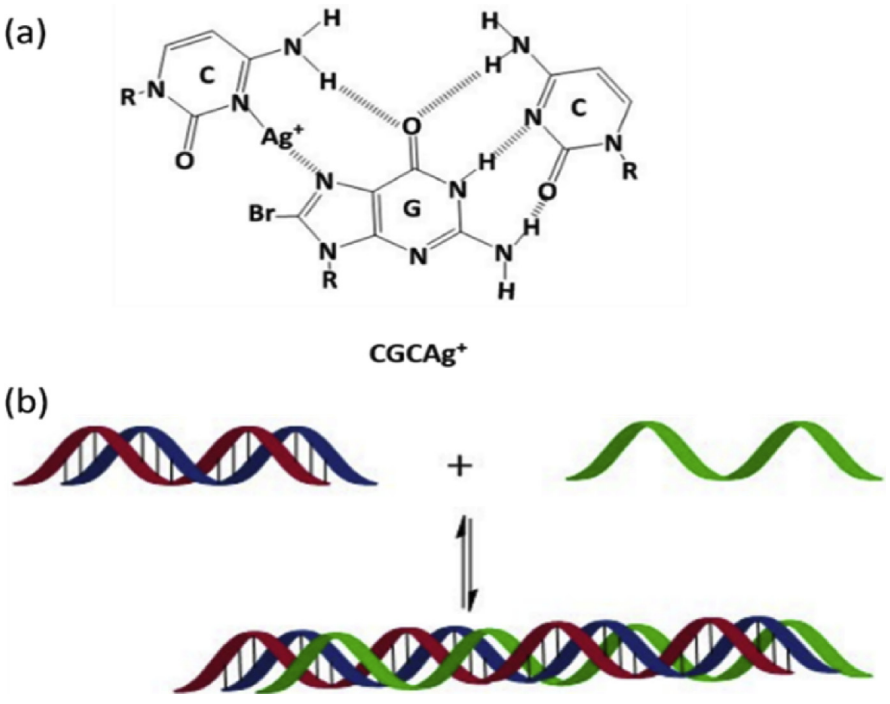

Fig. 5. Shows: (a) Triplexes structure of pyrimidine parallel motif CGC bases with Ag(I) ion. (b) Triplexes block of CGCAg+.displaying that the location of the third strand (green colour) is in the major groove of the double helix (red & blue colures) that is built via Hoogsteen hydrogen bonding.

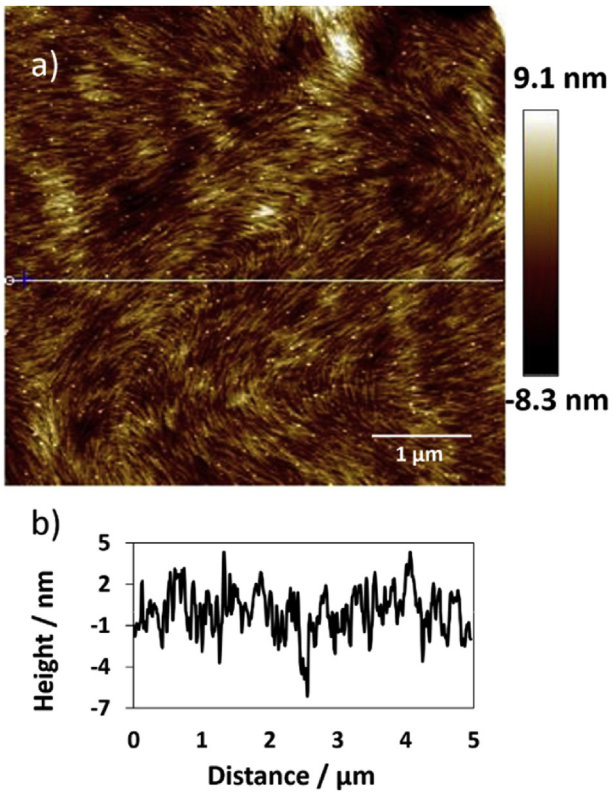

Fig. 6. (a)Tapping mode height AFM image (scan area 5 × 5 μm^2) of the Ag (I): mixture nucleosides polymer, shows the height of the polymer was in the range of 2–3 nm with very few peaks with height up to 5 nm. (b) The profile associated with the horizontal white line along image (a) showing the height of the fibres. The white dots in image (a) refer to the loops that formed by Watson-Crick and Hoogsteen hydrogen bonding.

2.4. Transmission electron microscopy (TEM) measurements

TEM measurements were carried out by using Philips CM100 electron microscope at accelerating voltage 100 kV. 2 µL of the sample was dropped onto a carbon coated copper grid, the sample was left to dry by air overnight before imaging.

2.5. Surface texture parameters analysis

Gwyddion software program was used to analysis AFM images.

2.6. Synthesis of derivative nucleoside: 8-bromo guanosine

8-Bromoguanosine was prepared according to the procedure of Srivastava [23]. N-Bromosuccinimide (0.4 g, 2.24 mmol) was added to the suspension of guanosine (0.566 g, 2 mmol in 16 mL anhydrous DMF) the suspension was constantly stirred for 24 h at room temperature. The resulting clear yellow solution was concentrated under reduced pressure to remove the solvent at 50 °C. The residue was collected by adding some water, followed by filtering the solid product and recrystallized by using hot water and drying by air (colourless crystal was yield (0.707 g with respect to the weight of guanosine, 80 %).

2.6.1. ^1H NMR characterization of 8-bromoguanosine

^1H NMR (300 MHz DMSO-*d6*, 25 °C) of guanosine spectrum in Fig. 2 showed: 10.63 δ (s, 1H, NH), 7.93 (s,1H, C8), 6.46 (s,2H, NH2), while ^1HNMR spectrum of 8-bromoguanosine in Fig. 3 displayed: δ 10.82 (s, 1H, NH), 6.55 (s, 2H, NH2). Disappearing the signal that belongs to (1H, C8) in Fig. 3 confirms successful preparation of 8-bromoguanosine.

2.7. Synthesis of polymer Ag(I): mixture nucleosides cytidine and 8-bromo guanosine

The one-dimensional (1D) polymer of Ag(I):cytidine and 8-bromoguanosine was prepared with stoichiometry 1:1:1 of Ag(I):cytidine:8-bromoguanosine as followed: The solution of 8-bromoguanosine (0.00615 gm, 16.98 µmol in 200 µL H_2O) was added to cytidine solution (0.00413 gm, 16.98 µmol in 100 µL DMSO), the mixture was shacked for several minutes then a solution of $AgNO_3$ (0.00288 gm, 16.98 µmol in 100 µL H_2O) was added, then the mixture was shacked quickly and left in a dark place at room temperature. After 30 min colourless viscose solution was formed, the viscosity of the sample was increased with the time. After four days of the preparation, the sample be more viscous, but it was not stable to inversion test to indicate the stability, and this confirms that the sample was not gel. 1.5 µL of the sample was drop-casted on a silicon chip and left to dry by air prior to scan by AFM.

3. Results and discussion

3.1. Preparation and characterization of Ag(I)-mixture nucleosides, cytidine and 8-bromoguanosine

The reaction of Ag(I) ions with equimolar equivalents mixture nucleosides, cytidine and 8-bromoguanosine, in aqueous solution leads to form triplex pyrimidine motif (Y), $CGCAg^+$, as shown in Fig. 4. The coordination of Ag(I) ion in the triplex CGC structure occurs via N3 atom of

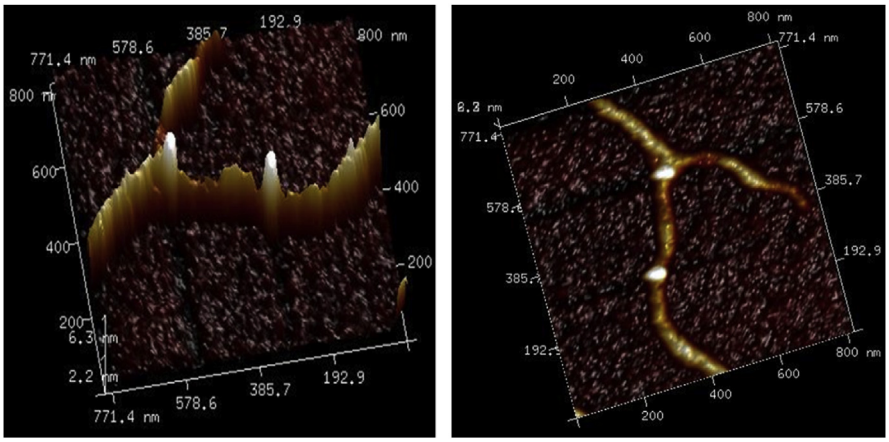

Fig. 7. Shows AFM images of the single polymer in 3D view to display the loops that formed in the triplex polymer.

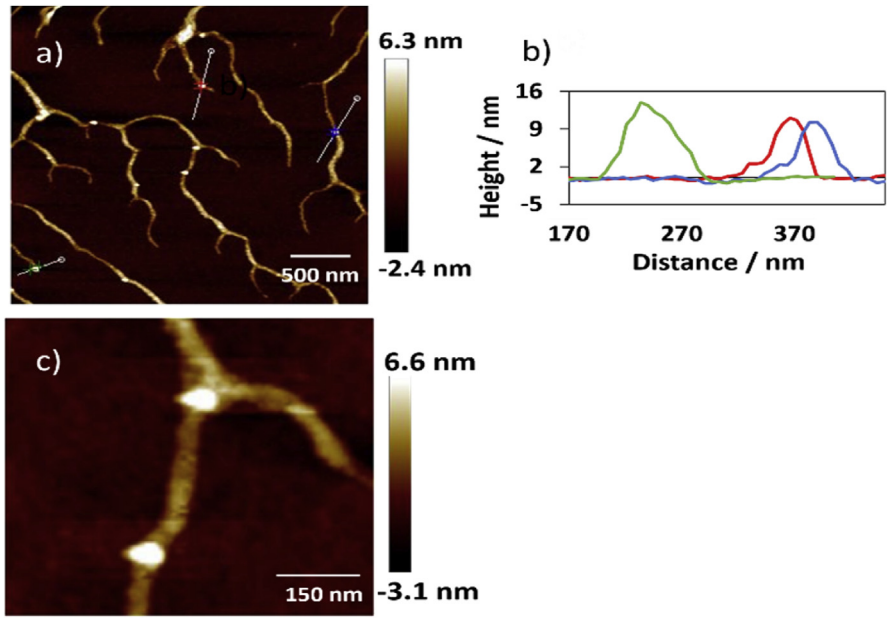

Fig. 8. Shows: (a) the height AFM image of the polymer with scale bar 500 nm, and (b) is the profile of the of the blue, red, and green lines across image (a) demonstrating the height of the loops that formed in the polymer, (c) small area of image (a) with scale bar 150 nm.

the cytidine molecular [24, 25], in fact, the presence of Ag(I) ions play fundamental role in the stability of the this structure [24, 26]. Protonation N3 atom in natural medium in cytidine molecular is necessary for complementarity binding with 8-bromoguanosine via Hoogsteen hydrogen bonding in CGC structure [27], this process provides appropriate site for coordinating Ag(I) ion to the cytidine molecular, and gives a rise to increase the stability of this structure, such protonation does not occur in the triplex GCG, and this confirms that the motif of the triplex structure of this fibrous polymer is CGC rather than GCG motif. The structure of the triplex Y motif in this polymer consists of two pyrimidine molecules (cytidine) and one purine molecular (8-bromoguanosine) to form $CGCAg^{+}$, purine and pyrimidine molecules are clustered in the same

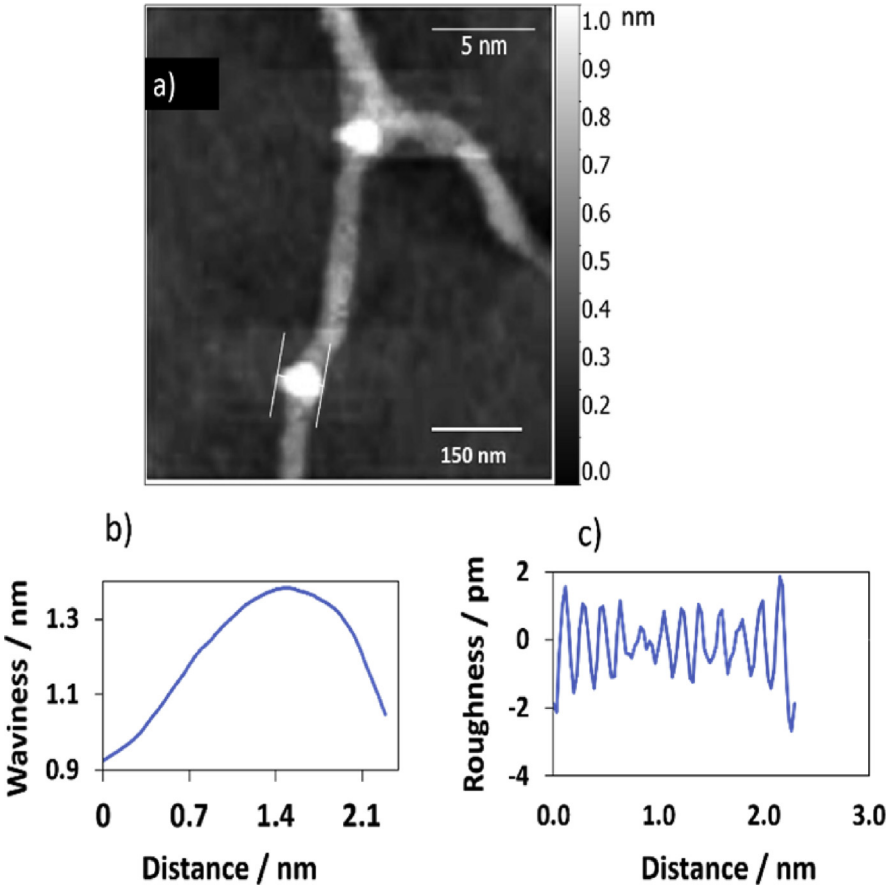

Fig. 9. (a) Tipping mode height AFM image with scale bar 150 nm of Ag(I): mixture cytidine and 8-bromoguanosine, the image was analysed by Gwyddion software program with scale 5 nm. The vertical bar that displayed on the right side of the AFM image is corresponding to the highest point (upper limit of the bar) and lowest points (lower point of the bar) that measured in the image in nanometre, respectively. The profiles of surface texture: waviness (b), and roughness (c) are associated with the sloping white lines in image (a).

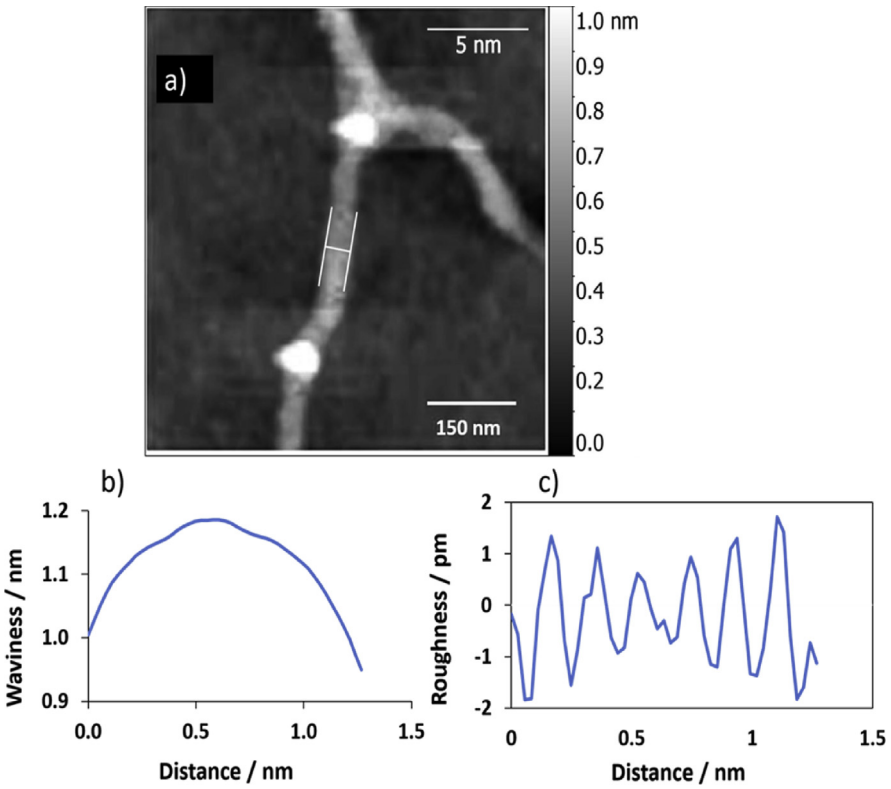

Fig. 10. Displays surface roughness parameters of the flat area of the single polymer of AFM image (a). (b) & (c) are the waviness and roughness profiles for the cross section in image (a). The scale bar was 5 nm.

strand by assisting of strand-switch mechanism.

Building triplex block of $CGCAg^{+}$ needs that the position of the third strand must be in the major groove of the double helix that is formed by Hoogsteen hydrogen bonding [27]. Triplexes structures of Y motif can be found in both RNA and DNA by forming intramolecular triplexes. Fig. 5 (a) showing the Triplet structure of parallel motif CGC bases with Ag(I)

Table 1
Statistical parameter values of the height distribution of AFM image in Fig. 9 (scanning area of 5 × 5 μm^2) for the 1D polymer Ag(I): mixture of nucleosides.

Parameter	Symbol	Value
Amplitude		
Roughness average	Ra	0.7 pm
Root mean square roughness	Rq	0.9 pm
Maximum height of the roughness	Rt	4.5 pm
Maximum roughness valley depth	Rv	2.7 pm
Maximum roughness peak height	Rp	1.9 pm
Average maximum height of the roughness	Rtm	2.7 pm
Average maximum roughness valley depth	Rvm	1.5 pm
Average maximum roughness peak height	Rpm	1.2 pm
Average third highest peak to third lowest valley height	R3z	2.7 pm
Average third highest peak to third lowest valley height	R3z ISO	0.9 pm
Average maximum height of the profile	Rz	2.7 pm
Average maximum height of the roughness	Rz ISO	2.7 pm
Skewness	Rsk	-0.256
Kurtosis	Rku	2.890
Waviness average	Wa	128.9 pm
Root mean square waviness	Wq	147.3 pm
Waviness maximum height	Wy = Wmax	1382.2 pm
Maximum height of the profile	Pt	1381.5 pm
Spatial		
Average wavelength of the profile	λa	0.20 nm
Root mean square (RMS) wavelength of the profile	λq	0.20 nm
Hybrid		
Average absolute slope	Δa	23.46 10-3
Root mean square (RMS) slope	Δq	28.89 10-3
Length	L	2.32 nm
Developed profile length	L0	2.32 nm
Profile length ratio	Ir	1.077

Table 2
Statistical parameter values of the height distribution of AFM image in Fig. 10 (scanning area of 5 × 5 μm^2) of the 1D polymer Ag(I): mixture of nucleosides.

Parameter	Symbol	Value
Amplitude		
Roughness average	Ra	0.8 pm
Root mean square roughness	Rq	0.9 pm
Maximum height of the roughness	Rt	3.6 pm
Maximum roughness valley depth	Rv	1.8 pm
Maximum roughness peak height	Rp	1.7 pm
Average maximum height of the roughness	Rtm	2.5 pm
Average maximum roughness valley depth	Rvm	1.4 pm
Average maximum roughness peak height	Rpm	1.1 pm
Average third highest peak to third lowest valley height	R3z	2.9 pm
Average third highest peak to third lowest valley height	R3z ISO	0.0 pm
Average maximum height of the profile	Rz	2.6 pm
Average maximum height of the roughness	Rz ISO	2.5 pm
Skewness	Rsk	0.166
Kurtosis	Rku	2.217
Waviness average	Wa	50.6 pm
Root mean square waviness	Wq	62.0 pm
Waviness maximum height	Wy = Wmax	1185.5 pm
Maximum height of the profile	Pt	1185.6 pm
Spatial		
Average wavelength of the profile	λa	0.20 nm
Root mean square (RMS) wavelength of the profile	λq	0.19 nm
Hybrid		
Average absolute slope	Δa	25.31 10-3
Root mean square (RMS) slope	Δq	31.39 10-3
Length	L	1.30 nm
Developed profile length	L0	1.30 nm
Profile length ratio	Ir	1.077

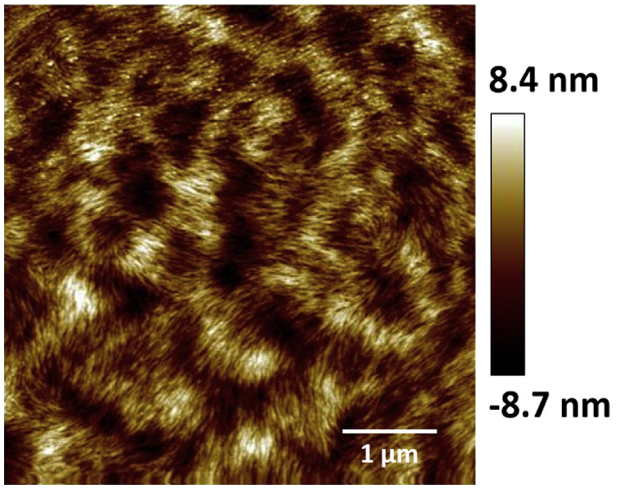

Fig. 11. Displays tapping mode height AFM image with scale bar 1 μm (scan area 5 × 5 μm^2) for the polymer of Ag(I): mixture nucleosides. This image was analysed using Gwyddion software program to obtain surface parameters.

ion, while Fig. 5 (b), modified from Sugimoto [28], displays building the triplex block, the green strand represents the third strand that be in the major groove of the double strands. Substitution C8 in guanosine [13, 15, 29, 30] molecular in Y motif can increase the stability of the triplex structure in addition to the stability that produces from the presence of Ag(I) ions and the influence of Hoogsteen hydrogen bonding in this structure. Most triplexes structures that concern RNA are synthesised regarding functionally RNAs such as ribosomal RNAs [31], telomerase RNAs [32], and long noncoding RNAs [33, 34]. In addition, these materials played a great role in molecular biology [35] and nanotechnology applications [36, 37].

Table 3
Statistical parameter values of the height distribution of AFM image (a) in Fig. 12 in the main text (scanning area of 5 × 5 μm^2) of the 1D polymer Ag(I): mixture of nucleosides.

Parameter	Symbol	Value
Amplitude		
Roughness average	Ra	1.3 pm
Root mean square roughness	Rq	1.7 pm
Maximum height of the roughness	Rt	10.4 pm
Maximum roughness valley depth	Rv	4.8 pm
Maximum roughness peak height	Rp	5.6 pm
Average maximum height of the roughness	Rtm	6.4 pm
Average maximum roughness valley depth	Rvm	3.1 pm
Average maximum roughness peak height	Rpm	3.3 pm
Average third highest peak to third lowest valley height	R3z	8.7 pm
Average third highest peak to third lowest valley height	R3z ISO	4.6 pm
Average maximum height of the profile	Rz	8.8 pm
Average maximum height of the roughness	Rz ISO	6.4 pm
Skewness	Rsk	-0.072
Kurtosis	Rku	3.865
Waviness average	Wa	49.9 pm
Root mean square waviness	Wq	59.4 pm
Waviness maximum height	Wy = Wmax	1176.2 pm
Maximum height of the profile	Pt	1176.5 pm
Spatial		
Average wavelength of the profile	λa	0.16 nm
Root mean square (RMS) wavelength of the profile	λq	0.16 nm
Hybrid		
Average absolute slope	Δa	0.05044
Root mean square (RMS) slope	Δq	0.06678
Length	L	5.96 nm
Developed profile length	L0	5.97 nm
Profile length ratio	Ir	1.033

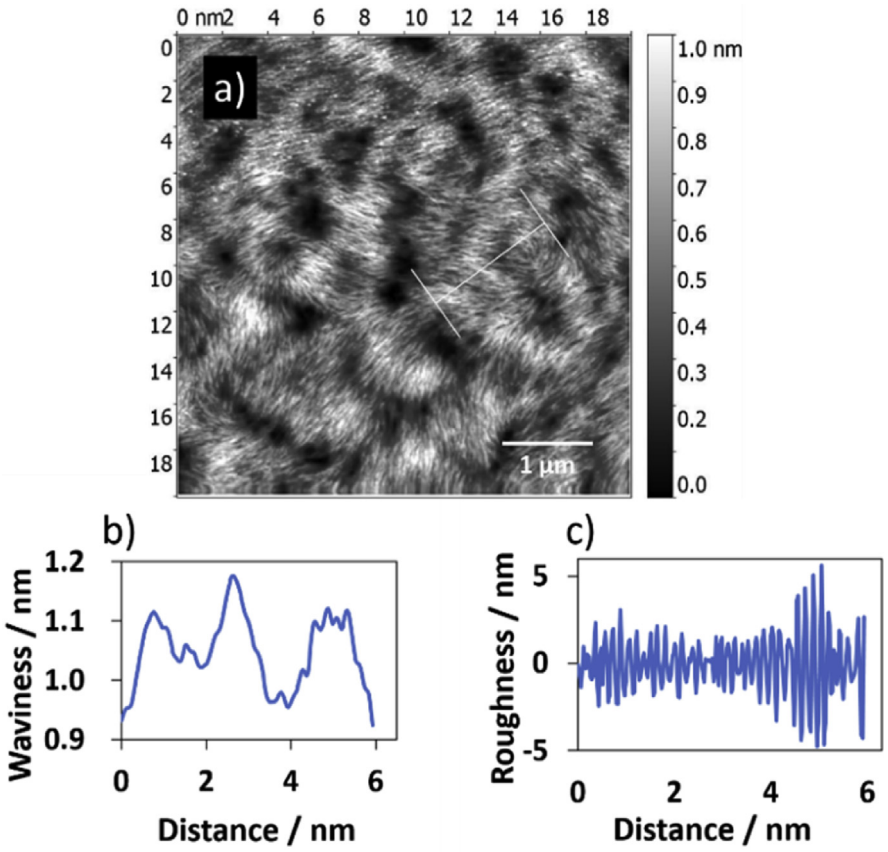

Fig. 12. Shows (a) surface analysis of AFM image (a) (scan area 5 × 5 μm^2). The vertical bar that displayed on the right side of the AFM image is corresponding to the highest point (upper limit of the bar) and lowest points (lower point of the bar) that measured in the image in nanometre, respectively, by using Gwyddion software program. The profiles of surface texture: waviness (b), and roughness (c) are the profile of the sloping white line in the AFM image (a). Selected line: (11.39, 11.64) to (16.19, 8.15) nm.

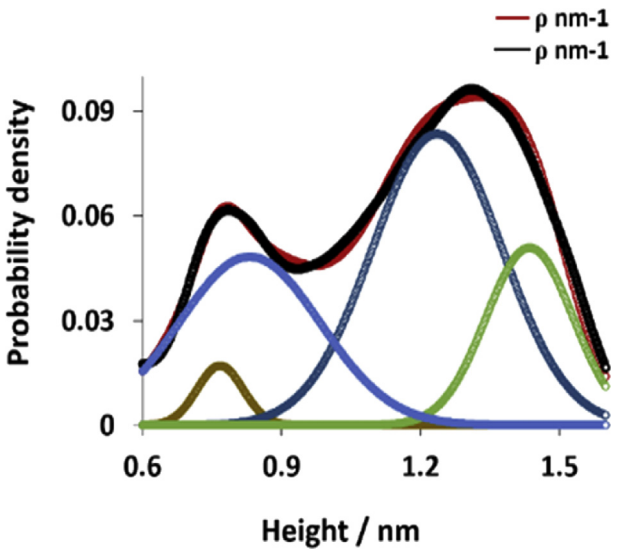

Fig. 13. Shows fibre high distribution for the polymer. The black line is a fitted regression model with a sum of four Gaussian functions, while the coloured lines displayed the individual Gaussians.

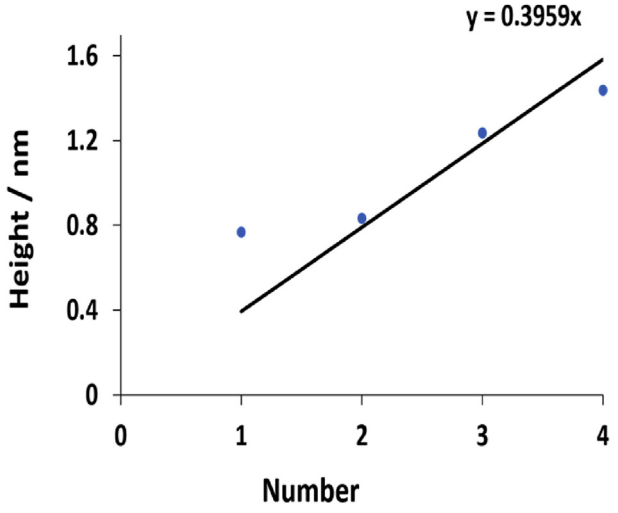

Fig. 14. Displays fibre diameter (size distribution) estimated from the peaks heights in Fig. 13. The data shows that the diameter was ~0.4 nm.

3.2. Atomic force microscopy (AFM) for surface characterization

The AFM technique was used to address the morphology of the polymer. Examination the dried polymer revealed formation of nanofibres extending many microns in length with a height in range of 2–3 nm, some few fibres revealed with height up to 4 nm. Fig. 6 displays tapping mode height AFM image that obtained by scanning area 5 × 5 μm^2. Many loops can be seen in image (a), Fig. 6 that formed as a consequent of binding of these complementary nucleosides. Fig. 7 displays more AFM images with 3D view for those loops that formed in the triplex polymer. Statistical analysis was carried out to investigate the height of the loops that can be seen in a single polymer in AFM image (a) in Fig. 8. The data displayed that the height values were in the range of 10–14 nm, as shown in Fig. 8 (b) which represents the profile of the three sloping lines in the image (a). Image (c) in Fig. 8 is a small area of image (a) with scale bar 150 nm. These findings indicate that the complementary binding cytidine and 8-bromoguanosine, that formed triplexes structures of parallel pyrimidine $CGCAg^{+}$, can self-assemble to form nanofibres. Self-assembling of nucleosides was seen for guanosine and its derivatives. Different architectures structures such as cyclic [38], lamellae [39], fibres [40], micelles [41], and films [42] have been reported for self-assembling of some complementary nucleobases and their derivatives. However, this is the first report that presents a simple and direct way to prepare nanofibers by self-assembling complementary nucleosides cytidine & 8-bromoguanosine.

3.3. Surface texture parameters analysis: waviness, and roughness statistical values of single polymer

Surface texture analysis is very useful to understand the nature of the material, and it helps in the development of many material components. The surface sample parameters of waviness and roughness of the single polymer were carried out for the AFM image with scanning area 5 × 5 μm^2 by using Gwyddion software program, the data are presented in Fig. 9 (for the loops) and Fig. 10 for the flat part of the single polymer. The data of Fig. 9 shows that the root mean square roughness (Rq) was 0.9 pm, and the roughness average was 0.7 pm. The Rq parameter, which is related to the standard division of the height distribution of the sample surface, has a special importance as it is more accurate than the average of height arithmetic (Ra), it calls also average roughness, owing to the high value of the deviation from the main line [43, 44]. Eq. (1) can be defined the Rq as:

$$RMS = R_q = \sqrt{\frac{1}{L}\int_0^L Z^2 \partial x} \approx \sqrt{\frac{1}{n}\sum_i^n Z_i^2} \quad (1)$$

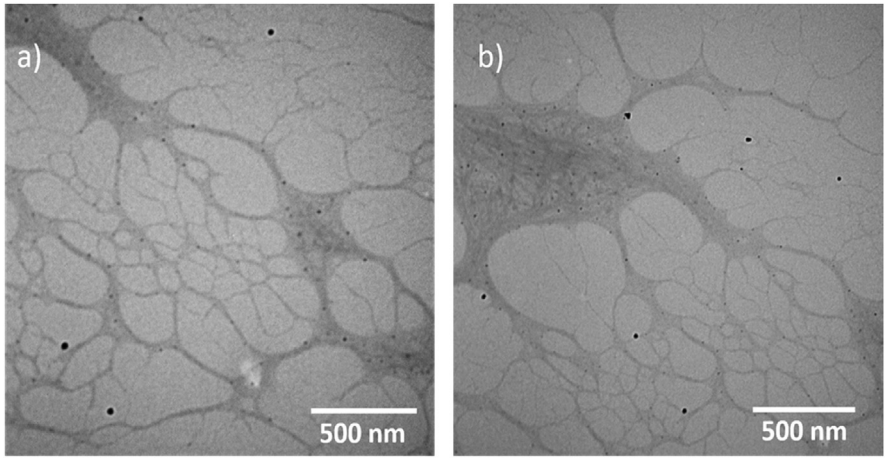

Fig. 15. Shows TEM images of the 1D polymer of Ag(I): mixture nucleosides, the scale bar was 500 nm in both images (a) and (b) while the magnification was 46000x and 34000x, respectively.

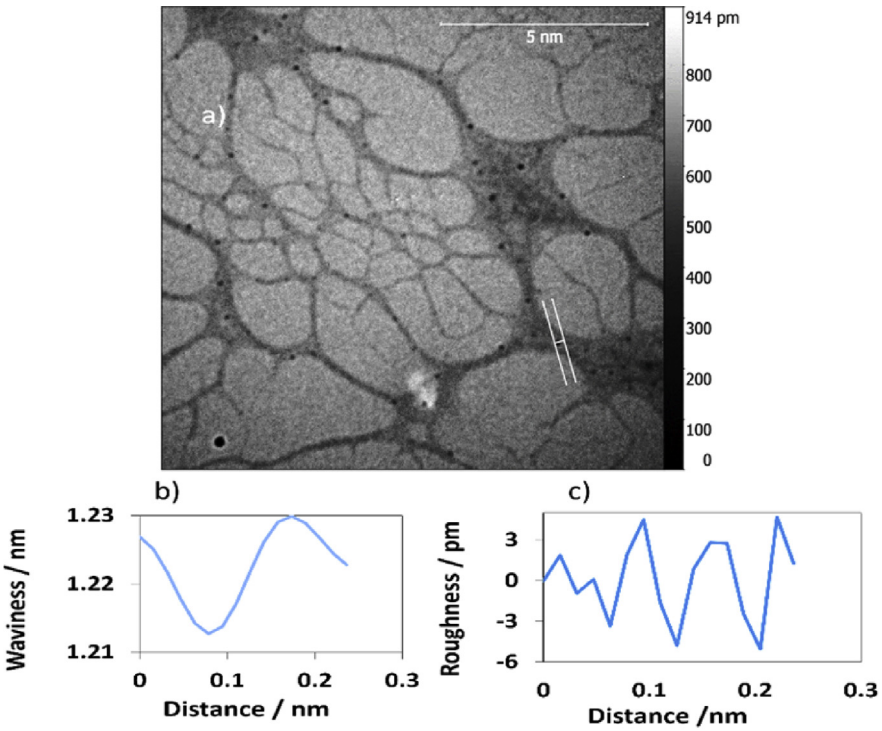

Fig. 16. (a) TEM image analysis,(b) & (c) are the waviness and roughness profiles for the cross section a long image (a). The scale bar was 5 nm.

RMS is the root mean square average deviation of the roughness, it is known as Rq, also. L and Z (x) are the length of the profile and the function of height profile, respectively. The data demonstrated that the root mean square waviness (Wq) was 147.3 pm, while the waviness average (Wa) was 128.9 pm. The height of the waviness is normally higher than the average roughness height by three times [43]. Tables 1 and 2 summarised the data of Figs. 9 and 10, respectively.

3.4. Kurtosis parameter

Kurtosis parameter describes the height distribution of the surface [45], the data in Table 1 shows that the value of Kurtosis was 2.89, and this confirms that the distribution curve has low height peaks and the morphology of the loop in the AFM image is valley rather than platy-kurtic valley, and this observation is very important as it gives a good

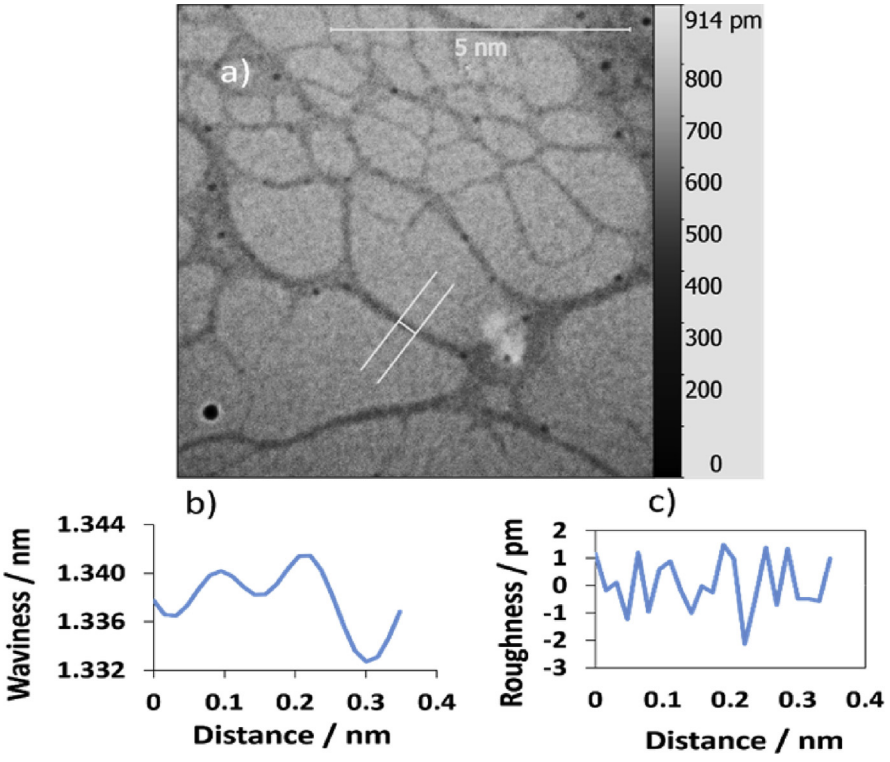

Fig. 17. Shows: (a) TEM image surface analysis, (b) & (c) are waviness & roughness profiles of the flat area of the single polymer in image (a). The scale bar was 5 nm.

Table 4
Statistical parameter values of the height distribution of TEM image in Fig. 16 in the main text (scanning area of 5 × 5 μm^2) of the 1D polymer Ag(I): mixture of nucleosides.

Parameter	Symbol	Value
Amplitude		
Roughness average	Ra	0.8 pm
Root mean square roughness	Rq	1 pm
Maximum height of the roughness	Rt	3.6 pm
Maximum roughness valley depth	Rv	2.1 pm
Maximum roughness peak height	Rp	1.5 pm
Average maximum height of the roughness	Rtm	1.7 pm
Average maximum roughness valley depth	Rvm	0.7 pm
Average maximum roughness peak height	Rpm	1 pm
Average third highest peak to third lowest valley height	R3z	2.3 pm
Average third highest peak to third lowest valley height	R3z ISO	0.0 pm
Average maximum height of the profile	Rz	2.6 pm
Average maximum height of the roughness	Rz ISO	1.7 pm
Skewness	Rsk	-0.196
Kurtosis	Rku	2.330
Waviness average	Wa	2 pm
Root mean square waviness	Wq	2.5 pm
Waviness maximum height	Wy = Wmax	1341.4 pm
Maximum height of the profile	Pt	1342.4 pm
Spatial		
Average wavelength of the profile	λa	0.06 nm
Root mean square (RMS) wavelength of the profile	λq	0.06 nm
Hybrid		
Average absolute slope	Δa	0.07958
Root mean square (RMS) slope	Δq	0.09789
Length	L	0.36 nm
Developed profile length	L0	0.37 nm
Profile length ratio	Ir	1.009

estimation about the nature of the surface roughness of the polymer. Low peaks are expected to be found in the distribution curve when the value of this parameter <3 and vice versa [45].

3.5. Surface polymer analysis using surface roughness parameters

Gwyddion software program was used to obtain surface roughness parameters by analysis the tapping mode height AFM image, Fig. 11, with scale bar 1 μm (scan area 5 × 5 μm^2) for the polymer of Ag(I): mixture nucleosides. The image was adjusted to greyscale for analysis, as shown in Fig. 12(a). The scale of the chosen line was 5 nm. Table 3 displays the data that obtained for analysis AFM image (a) in Fig. 12. The data shows that the value of the Kurtosis was >3 and this indicates that the distribution curve is platykurtic rather than a valley [45]. On the other hand, the data showed that the value of Ra (1.3) is less than Rq (1.7) by ~ 30 %, and this confirms that the roughness profile is following Gaussian distribution [46, 47]. For Gaussian surface; Rq and Ra are interchangeable as shown in Eq. (2):

$$R_q \sim \sqrt{\frac{\pi}{2}} Ra \sim 1.25 \times R_a \quad (2)$$

The height distribution of the AFM image (a) in Fig. 12 is fitted to a sum of Gaussian functions to obtain the probability density of the fibres, as shown in Fig. 13, and the straight line in Fig. 14 is fitted through the peak (height) values to get an estimate of ~0.4 nm diameter for the fibres.

3.6. Transmission electron microscopy (TEM)

TEM technique was used to investigate the morphology of the polymer. Carbon coated copper grid was used as a substrate to prepare the sample. 1.5 μL of the sample was drop-casted onto the substrate, left to dry by air prior to imaging. The inspection revealed the formation of a very long, entangled fibres, as shown in Fig. 15. The surface of the single polymer was investigated for the TEM images by using Gwyddion software program to obtain parameters of waviness and roughness, Figs. 16 and 17 display the data for the loops and for the flat part of the single polymer, respectively. Table 4 presents the data of Fig. 16. The data shows that the root mean square roughness (Rq) was 1.0 pm, and the roughness average was 0.8 pm. In addition, the value of Kurtosis (Rku) was 2.33. The data of TEM images were in a good agreement with that of AFM images and this confirms the accurate measurements for analysis the surface texture of the triplex polymer CGCAg$^+$.

4. Conclusions

In summary, one dimensional triplex parallel pyrimidine polymer of Y motif based on self-assemble of Ag(I) with mixture complementary bases nucleosides (G & C) was prepared, to the best of our knowledge, this is the first report displays that complimentary nucleosides, cytidine & 8-bromoguanosine, are capable of self-assembling directly to produce nanostructure material with such length and height as shown by AFM measurements where the height of the polymer was in the range of 2–3 nm and the length was many microns. This feature makes this polymer analogous to the duplex DNA [4]. Surface roughness was carried out to indicate the probability density of the fibre. The data displayed that the diameter of the fibre was ~0.4 nm. Waviness, Roughness, and Kurtosis parameter values for the fibrous structure were also investigated by analysis AFM images and TEM images where the data showed a good agreement.

Declarations

Author contribution statement

Lamia al-Mahamad: Conceived and designed the experiments; Performed the experiments; Analyzed and interpreted the data; Contributed reagents, materials, analysis tools or data; Wrote the paper.

Funding statement

This research did not receive any specific grant from funding agencies in the public, commercial, or not-for-profit sectors.

Competing interest statement

The authors declare no conflict of interest.

Additional information

No additional information is available for this paper.

References

[1] L. Liu, F. Besenbacher, M. Dong, Self-Assembly of DNA bases via hydrogen bonding studied by scanning celing microscopy, Nucleic Acids Mol. Biol. 29 (2014).
[2] Z.-T. Li, L.-Z. Wu, Hydrogen Bonded Supramolecular Structures, in: D.-W. Zhang, H. Wang, Z.-T. Li (Eds.), Chapter 1. Hydrogen Bonding Motifs: New Progresses, vol. 87, Springer-Verlag GmbH Berlin Heidelberg, 2015.
[3] K. Araki, I. Yoshikawa, Nucleobase-containing gelators, Top. Curr. Chem. 256 (2005) 133–165.
[4] L.L.G. Al-Mahamad, O. El-Zubir, D.G. Smith, B.R. Horrocks, A. Houlton, A coordination polymer for the site-specific integration of semiconducting sequences into DNA-based materials, Nat. Commun. 8 (2017) 720.
[5] P. Amo-Ochoa, S. Verma, J. Kumar, F. Zamora, Semiconductive and magnetic one-dimensional coordination polymers of Cu(II) with modified nucleobases, Inorg. Chem. 52 (2013) 11428–11437.
[6] A. Kumar, S.K. Gupta, Supramolecular-directed novel superparamagnetic 5′-adenosine monophosphate templated β-FeOOH hydrogel with enhanced multi-functional properties, Green Chem. 17 (2015) 2524–2537.
[7] D. Jonckheere, J. Hofkens, M.B.J. Roeffaers, D.E. De Vos, Silver-induced reconstruction of an adeninate-based metal–organic framework for encapsulation of luminescent adenine-stabilized silver clusters, J. Mater. Chem. C 4 (2016) 4259–4268.

[8] C.S. Purohit, S. Verma, A luminescent silver-adenine metallamacrocyclic quartet, J. Am. Chem. Soc. 128 (2006) 400–401.

[9] J. Thomas, SupraMOFs: Supramolecular Porous Materials Assembled from Metal–Nucleobase Discrete Entities, Thesis. University of the Basque Country, 2015.

[10] P. Amo-Ochoa, F. Zamora, Coordination polymers with nucleobases: from structural aspects to potential applications, Coord. Chem. Rev. 276 (2014) 34–58.

[11] V. Abet, R.l. Rodriguez, Guanosine and isoguanosine derivatives for supramolecular devices, New J. Chem. 38 (2014) 5122–5128.

[12] B. Adhikari, A. Shah, H.-B. Kraatz, Self-assembly of guanosine and deoxy-guanosine into hydrogels: monovalent cation guided modulation of gelation, morphology and self-healing properties, J. Mater. Chem. B 2 (2014) 4802–4810.

[13] J.L. Sessler, K. Doerr, V.V. Lynch, K. Abboud, A G-quartet formed in the absence of a templating metal cation: a new 8-(N,N-dimethylaniline)guanosine derivative this work was supported by the robert a. Welch foundation, Angew Chem. Int. Ed. Engl. 39 (2000) 1300–1303.

[14] T. Bing, W. Zheng, X. Zhang, L. Shen, X. Liu, F. Wang, J. Cui, Z. Cao, D. Shangguan, Triplex-quadruplex structural scaffold: a new binding structure of aptamer, Sci. Rep. 7 (2017) 15467.

[15] R.N. Das, Y.P. Kumar, S. Pagoti, A.J. Patil, J. Dash, Diffusion and birefringence of bioactive dyes in a supramolecular guanosine hydrogel, Chem. Eur J. 18 (2012) 6008–6014.

[16] L. Mistry, O. El-Zubir, G. Dura, W. Clegg, P.G. Waddell, T. Pope, W.A. Hofer, N.G. Wright, B.R. Horrocks, A. Houlton, Addressing the properties of "Metallo-DNA" with a Ag(i)-mediated supramolecular duplex, Chemical Science, 2019.

[17] G.A. Somorjai, Y. Li, Impact of surface chemistry, Proc. Natl. Acad. Sci. Unit. States Am. 108 (2010) 917–924.

[18] R.J. Kline, D.M. DeLongchamp, D.A. Fischer, E.K. Lin, Significant dependence of morphology and charge carrier mobility on substrate surface chemistry in high performance polythiophene semiconductor films, Appl. Phys. Lett. 90 (2007).

[19] M.S. Shur, R. Gaska, Wide Energy Bandgap Electronic Devices. Chapter 3. GaN-Based Power High Electron Mobility Transistors, World Scientific Publishing Co. Pte. Ltd., 2003.

[20] S. Michael, L. Lianghong, F.M. John, P. Tania, Growth Technology for GaN and AlN Bulk Substrates and Templates from: Handbook of GaN Semiconductor Materials and Devices Routledge, 2017.

[21] J.G. Ekerdt, Y.M. Sun, A. Szabo, G.J. Szulczewski, J.M. White, Role of surface chemistry in semiconductor thin film processing, Chem. Rev. 96 (1996) 1499–1518.

[22] J. Ren, Micro/nano Scale Surface Roughness Tailoring and its Effect on Microfluidic Flow, Iowa State University, 2013. PhD Thesis.

[23] P.C. Srivastava, K.L. Nagpal, Bromination of nucleosides, Experientia 26 (1970) 220.

[24] S. Urata, T. Miyahata, H. Matsuura, Y. Kitamura, T. Ihara, Alteration of DNAzyme activity by silver ion, Chem. Lett. 43 (2014) 1020–1022.

[25] T. Ihara, T. Ishii, N. Araki, A.W. Wilson, A. Jyo, Silver ion unusually stabilizes the structure of a parallel-motif DNA triplex, J. Am. Chem. Soc. 131 (2009) 3826–3827.

[26] K. Tanaka, Y. Yamada, M. Shionoya, formation of silver(I)-Mediated DNA duplex and triplex through an alternative base pair of pyridine nucleobases, J. Am. Chem. Soc. 124 (2002) 8802–8803.

[27] M.D. Frank-Kamenetskii, S.M. Mirkin, Triplex DNA structures, Annu. Rev. Biochem. 64 (1995) 65–95.

[28] N. Sugimoto, P. Wu, H. Hara, Y. Kawamoto, pH and cation effects on the properties of parallel pyrimidine motif DNA triplexes, Biochemistry 40 (2001) 9396–9405.

[29] A. Aviñó, M. Frieden, J.C. Morales, B.G. de la Torre, R. Güimil García, F. Azorín, J.L. Gelpí, M. Orozco, C. González, R. Eritja, Properties of triple helices formed by parallel-stranded hairpins containing 8-aminopurines, Nucleic Acids Res. 30 (2002) 2609–2619.

[30] R. Soliva, R. Güimil García, J.R. Blas, R. Eritja, J.L. Asensio, C. González, F.J. Luque, M. Orozco, DNA-triplex stabilizing properties of 8-aminoguanine, Nucleic Acids Res. 28 (2000) 4531–4539.

[31] P. Nissen, J.A. Ippolito, N. Ban, P.B. Moore, T.A. Steitz, RNA tertiary interactions in the large ribosomal subunit: the A-minor motif, Proc. Natl. Acad. Sci. U. S. A. 98 (2001) 4899–4903.

[32] C.A. Theimer, C.A. Blois, J. Feigon, Structure of the human telomerase RNA pseudoknot reveals conserved tertiary interactions essential for function, Mol. Cell. 17 (2005) 671–682.

[33] M. Szabat, E. Kierzek, R. Kierzek, Modified RNA triplexes: thermodynamics, structure and biological potential, Sci. Rep. 8 (2018) 13023.

[34] S.L. Moon, M.D. Barnhart, J. Wilusz, Inhibition and avoidance of mRNA degradation by RNA viruses, Curr. Opin. Microbiol. 15 (2012) 500–505.

[35] A. Bacolla, G. Wang, K.M. Vasquez, New perspectives on DNA and RNA triplexes as effectors of biological activity, PLoS Genet. 11 (2015), e1005696.

[36] D. Jasinski, F. Haque, D.W. Binzel, P. Guo, Advancement of the emerging field of RNA nanotechnology, ACS Nano 11 (2017) 1142–1164.

[37] A.R. Chandrasekaran, D.A. Rusling, Triplex-forming oligonucleotides: a third strand for DNA nanotechnology, Nucleic Acids Res. 46 (2018) 1021–1037.

[38] Y. Xin, X. Kong, X. Zhang, Z. Lv, X. Du, Self-Assembly and molecular recognition of adenine- and thymine-functionalized nucleolipids in the mixed monolayers and thymine-functionalized nucleolipids on aqueous melamine at the air–water interface, Langmuir 28 (2012) 11153–11163.

[39] K. Zhang, S.J. Talley, Y.P. Yu, R.B. Moore, M. Murayama, T.E. Long, Influence of nucleobase stoichiometry on the self-assembly of ABC triblock copolymers, Chem. Commun. 52 (2016) 7564–7567.

[40] C. Li, B.J. Cafferty, S.C. Karunakaran, G.B. Schuster, N.V. Hud, Formation of supramolecular assemblies and liquid crystals by purine nucleobases and cyanuric acid in water: implications for the possible origins of RNA, Phys. Chem. Chem. Phys. 18 (2016) 20091–20096.

[41] Y. Kang, A. Lu, A. Ellington, M.C. Jewett, R.K. O'Reilly, Effect of complementary nucleobase interactions on the copolymer composition of RAFT copolymerizations, ACS Macro Lett. 2 (2013) 581–586.

[42] C. Tang, S.-m. Hur, B.C. Stahl, K. Sivanandan, M. Dimitriou, E. Pressly, G.H. Fredrickson, E.J. Kramer, C.J. Hawker, Thin film morphology of block copolymer blends with tunable supramolecular interactions for lithographic applications, Macromolecules 43 (2010) 2880–2889.

[43] R.R.L.D. Oliveira, D.A.C. Albuquerque, T.G.S. Cruz, F.M. Yamaji, F.L. Leite, Measurement of the nanoscale roughness by atomic Force microscopy: basic principles and applications, in: Dr. Victor Bellitto (Ed.), Atomic Force Microscopy - Imaging, Measuring and Manipulating Surfaces at the Atomic Scale, InTech, 2012. Available from: http://www.intechopen.com.

[44] F.G. Echeverrigaray, S.R.S.d. Mello, L.M. Leidens, C.A. Figueroa, Towards superlubricity in nanostructured surface: the role of van der waals Force, Phys. Chem. Chem. Phys. (2018).

[45] P.J.R. Torregrosa, Study of Structured Surfaces from Micro-to Nano-Scale Topography for Bioadhesive Applications, PhD thesis, University of Granada, 2015.

[46] S.M. Tavares, Analysis of Surface Roughness and Models of Mechanical Contacts, Thesiss, Facoltà di Ingegneria – Università di Pisa, Italy, 2005.

[47] B. Bhushan, Surface Roughness Analysis and Measurement Techniques, Chapter 2, The Ohio State University. CRC Press LLC, 2001.